2006

A Theoretical Model and Experimental Validation of a Sliding Vane Rotary Compressor

Roberto Cipollone
University of L'Aquila

Giulio Contaldi
Ing. Enea Mattei

Antonio Sciarretta
University of L'Aquila

Raffaele Tufano
Ing. Enea Mattei

Carlo Villante
University of L'Aquila

A THEORETICAL MODEL AND EXPERIMENTAL VALIDATION OF A SLIDING VANE ROTARY COMPRESSOR

Roberto CIPOLLONE[1], Giulio CONTALDI[2]
Antonio SCIARRETTA[1], Raffaele TUFANO[2], Carlo VILLANTE[1]

[1] University of L'Aquila, DIMEG
L'Aquila (AQ), Italy
(++39.862.434319, robcip@ing.univaq.it)
[2] Ing. Enea Mattei S.p.A.
Vimodrone (MI), Italy
(+39 02 253051, giulio_contaldi@mattei.it)

ABSTRACT

The authors have developed [1] a comprehensive model for SVRC machines based on a suitable expression of the conservation laws, modeling together with the internal transformations the air dynamics in suction and discharge circuits, including transient and wave propagation effects. Non-conventional complex processes have also been included (oil/air saturation, oil/air separation, characteristic heat transfer, etc.), in order to closely represent the real behaviour. A further improvement is presented in this paper: the oil circulation model has been included, a dynamic modeling of the blade orientation inside the rotor slot as well as a modeling for the power absorbed due to friction.
A specific test bench has been built to validate the effectiveness of the overall modeling, in terms of the conventional performance parameters as well as more machine dependent quantities.

1. INTRODUCTION

Sliding vane rotary compressors (SVRC) represent a class of machines which show inherent advantages with respect to the other different volumetric configurations, reciprocating as well as rotative. They share with these, a rather constant air delivery rate as a function of discharge pressure and a mass flow rate strictly dependent on the speed of rotation. With respect to these, the SVRC are able to give a very low specific energy consumption per unit mass of air inducted, with a significant potential of consumption reduction in the case of high power machines, having typical values in the order of 5-6 kW/(m^3/min). Moreover, the reliability represents a known key aspect, especially appreciated for industrial high duty applications. Over the centrifugal compressors, the SVRC are quieter, don't suffer of vibrations and pulsating mass flow delivery, a favorable weight to power ratio, a constant pressure level auto regulated by the discharge line.
Of course, some drawbacks of the SVRC machines should also be mentioned. If one compares the SVRC with the other volumetric rotary compressors (screw, etc...) they have greater lubricating oil circulation, need more specific oil properties and the constructional tolerances and superficial finishing must be strictly under control.
SVRCs have been long studied in terms of geometrical characteristics, to improve performance by optimizing some design parameters (number of blades, blade inclination, shape of the stator, rotor radius, etc.), and in terms of the forces exchanged at the various contact points between the machine parts (2-5).
However, the evaluation of the machine performance additionally requires a thermodynamic model to calculate how the pressure varies in the cells as a function of time. This calculation is strongly coupled with the fluid dynamics modeling of suction, discharge, and oil circuits, particularly when the compressor is part of a multi-component energy system. This being such a complex task, a system modeling approach has been often neglected in literature works (2-5).
As already observed (1) a comprehensive model has been presented which matches the geometrical and thermodynamical aspects but neglects the transient behaviour at the suction and discharge ports, this being one of the most important aspects to represent the machine as part of a real compressed air installation. The oil circulation as well as the vibrating behaviour of the blades have also been neglected representing key aspects of the machine behaviour. The authors already developed a comprehensive model including the dynamics of the inlet and outlet, making use of a suitable fluodynamic approach, (6).

In this paper oil circulation and blade vibration have been added to the model making reference to a realistic injection oil system (pressure rail, filter, orifices, etc) as well as to a realistic blade in rotor slot configuration. The blade setting inside the slot has required the evaluation of the equilibrium forces, so a modeling of the friction and of the power absorbed due to it is has been also presented. This to progress towards a fine tuned design tool strictly based on sound physical consistency.
In addition a dedicated test bench has been built whose results have been used to validate the effectiveness of the overall modeling.

2. GEOMETRIC MODEL

A detailed geometrical description of the machine is performed taking into consideration all the main dimensions typical of a SVRC. The complete description can be found in (5). This also includes non conventional geometries such as non circular stators and rotors, inclined blades, etc. as well as other parameters which approach the description to typical real situations. Used as a design tool, the model also evaluates any geometrical conflicts which can easily arise when examining new SVRC designs. The core of the geometrical sub-model is the evaluation of the volume V of a cell as a function of the angle of rotation of its leading blade
Particular attention has been given to the inlet and outlet ports, where there exists important fluodynamic phenomena concerning intake and discharge which are taken into consideration in the model.
In real SVRCs, the passage areas may be located on the lateral surface of the stator leading to a radial intake/exhaust flow or on the frontal surface of the stator leading to an axial intake/exhaust flow. In the first case the ports are usually located on the stator surface, as a series of slots having a total length L_d (generally smaller than the rotor/stator length L). The position of the slots on the stator circumference is usually defined by two angles; the passage area is then obtained making reference to them. In the second case the evaluation of the port passage area is more complex and must be calculated as the superposition of the cell area and the port surface. The model chooses a suitable way for representing these two quantities hence appropriately assigning the visible port area to all the cells overlapping the ports at any instant.

3. THERMODYNAMIC MODEL

The thermodynamic model of the air delivered by a SVRC consists of mass and energy conservation equations concerning the main thermodynamic properties of the air-oil mixture in each single cell. Each cell is described by a capacity whose volume varies with time according to the output of the geometrical sub-model. A cell capacity exchanges mass and energy with the other cells through the vane clearance and, if it is the case, with the suction and discharge circuits via the respective ports. Moreover, it exchanges energy with the external environment through the machine walls.
The conservation law of the mixture mass M is written as:

$$dm/dt = \sum \dot{m} \tag{1}$$

where the sum is extended to all the mass exchange paths i.e., the suction and discharge ports and the leakage between adjacent cells. The latter term is calculated assuming a linear dependency between pressure difference and mass flow rate (i.e., $\dot{m}_{leak} = k_{leak} \cdot \Delta p$).
The remaining mass flow rate terms are outputs of the fluid-dynamic sub-model. Similarly, the conservation law for the oil mass m_o is written as:

$$\frac{dm_o}{dt} = \sum \dot{m}_o + \dot{m}_{inj} - \dot{m}_{o,s} \tag{2}$$

where the $\dot{m}_{inj}$ is the oil mass flow rate injected, while $\dot{m}_{o,s}$ describes the saturated oil mass.
Oil mass, in fact, condenses when oil fraction is larger than the equilibrium fraction at the current mixture pressure and temperature, and may be therefore calculated as follows:

$$\dot{m}_{o,s} = m_o - m\left[f_{sat}(p,T) \cdot M_o \right] / \left[p \cdot M \right] \tag{3}$$

where the saturation pressure $f_{sat}(p,T)$ is a tabulated function of pressure and temperature. The mixture molar mass M is calculated by:

$$M = M_o M_a \Big/ \left[cM_a + (1-c) M_o \right] \tag{4}$$

where $c=m_0/m$ is the oil mass fraction.
Energy conservation law implies the evaluation of enthalpy flows associated with mixture flows ($\dot{m}h$), mechanical work ($-p \cdot \dot{V}$), heat flows ($\dot{q}$), latent heat of vaporization and condensation,

$$\frac{dU}{dt} = \sum \dot{m}h - \dot{q} - p \cdot \dot{V} + H_{LHV}(T) \cdot \left[\frac{dm_{o,s}}{dt} - \frac{dm_{inj}}{dt} \right] \tag{5}$$

Being U the internal energy of the gas inside the cell. The heat flow rate is calculated as proportional to the temperature difference between cell mixture and walls via a global heat coefficient χ_{hf}. This represents a simplified but practical way to describe the heat convection between the compressor casing and the environment, as well as the heat removed by the air. Finally, mixture temperature and pressure are updated using ideal gas properties

4. FLUID DYNAMIC MODEL

The mass and energy flows exchanged between the cells and the suction and discharge circuits, as well as between different parts of the same circuits, are evaluated using a general-purpose, lumped-parameter, fluid dynamics model, the QPM (6). Such a model calculates, in an unsteady way, the transport properties (mass flow rates, energies, etc…) and accounting for the capacitive inertial and propagative fluid dynamic phenomena. According to this approach the suction and discharge are represented including all the transient phenomena in the induction and discharge lines.

5. BLADE DYNAMIC MODELING

The dynamic blade sub-model calculates the friction power at the contact surfaces between blades, rotor, and stator. At most, there will be three contact points, whose position depends on the orientation taken by the blades as a consequence of the pressure difference between adjacent cells.
A fixed coordinate system where the slot is vertical and the rotation of the rotor is counterclockwise (Fig. 5) is taken as a reference. The angle θ is defined as the angle between the stator axis, the blade-stator contact point C_3, and the rotor axis. It is determined solely by the geometry and by the kinematics of the machine, so it can be calculated and stored for each rotor angle α. Fig 5 is a simple sketch which does not take into account the local geometries around the contact points. For sake of simplicity the equations used make reference to this rendition. Real geometries can be considered at a later stage without significant loss of validity of this model.
If θ is positive, as in Fig. 5(a), it means that the blade is entering the slot, i.e., the blade vertical velocity u_{blade} is negative. Otherwise, if θ is negative, the blade is leaving the slot and its vertical velocity is positive. The relative velocity between the blade and the slot is necessary to determine the orientation of the friction force at the contact points C_1 and C_2 between the blade and the rotor.
The friction forces are balanced by several other forces interesting the blade, which are represented in Fig. 5(b) for a given blade orientation. Namely, they are: F_1 the contact force in C_1; F_2 the contact force in C_2; F_c the centrifugal force, F_{pn} the force due to the differential pressure between the adjacent cells, F_{pb} the force due to the pressure difference between the blade base and the blade tip, F_w the contact force in C_3. Forces F_{pn} and F_{pb} are calculated at each time step from the pressure in the cells; force F_c is solely determined by the geometry of the machine and thus it is calculated at each time step as a function of the current value of α. The three unknown quantities to be calculated at each time step are thus the normal components of the forces F_1, F_2, and F_w. With reference to the situation in Fig 5(b), the force and momentum balances provide the three equations required as follows.

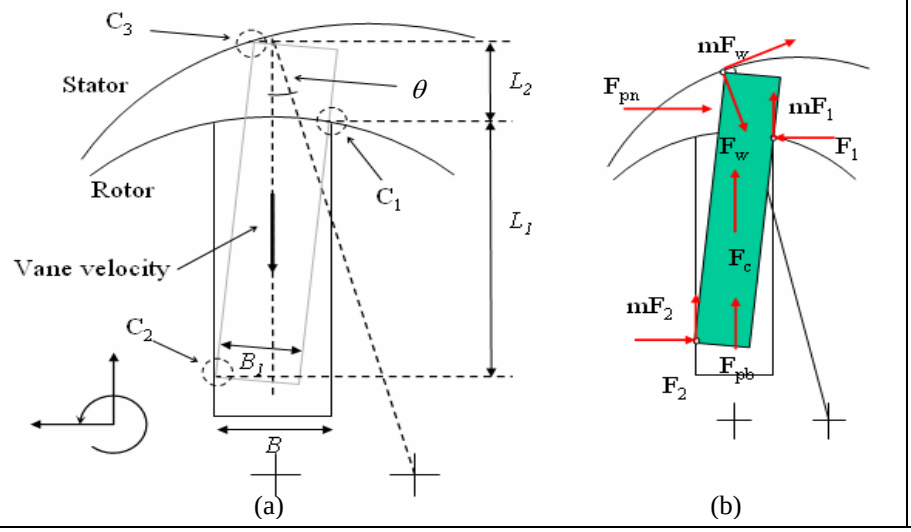

F_1: Reaction force
F_2: Reaction force
F_c: Centrifugal force
F_w: Reaction force
F_{pn}: Side to side diff. pressure force
F_{pb}: Tip to base diff. pressure force

Fig. 5 – Blade dynamical modeling

$$\begin{cases} \pm\left(\mu F_1 + \mu F_2\right) + k_1 F_w + F_{pb} + F_c = 0 \\ F_1 - F_2 - \left(\mu\cos\vartheta + \sin\vartheta\right) F_w - F_{pn} = 0 \\ F_2 L_1 \mp \mu F_2 B - \left(\mu\cos\vartheta + \sin\vartheta\right) F_w L_2 - k_1 F_w B_1 - F_{pn} L_2 / 2 - F_{pb} B_1 - F_c B_1 = 0 \end{cases} \tag{8}$$

the distances $\boldsymbol{L}_1$, $\boldsymbol{L}_2$, B and $\boldsymbol{B}_1$ are defined in Fig. 5, and $\pm$ is dependent upon the sign of θ. The given system is solved with standard linear algebra methods: the solution allows the calculation of the friction power as:

$$P_{fric} = \mu F_3 u_{per} + \mu\left(F_1 + F_2\right) u_{blade} \tag{9}$$

where u_{per} is the peripheral speed that depends on the rotational compressor speed. In general, the solution of the system can lead to negative contact forces: this means that that blade orientation is not achievable. Four possible blade orientations are considered in the model : The "backward tilt", *BT*, in which C_1 is on the leading side and C_2 on the trailing side; "hard backward", *HB*, with C_1 and C_2 both on the leading side; "forward tilt", *FT*, with C_1 on the trailing side and C_2 on the leading side; "hard forward", *HF*, with C_1 and C_2 both on the trailing side.
For the four cases, the model solves the system of equations (8), re-written for convenience in a matrix form as:

$$[A]\cdot[X] + [B] = 0 \tag{10}$$

where the unknown vector [*X*] comprises the three contact forces. The coefficients of the matrix [*A*] and of the vector [*B*] are shown in the Appendix for the four cases *BT*, *HB*, *FT*, and *HF*. In the case of multiple solutions the model chooses that with the lowest friction force. This gives a continuous blade orientation throughout a full rotation.

6 OIL CIRCULATION MODEL

The oil is injected inside the compressor by means of several in-line injectors; the backpressure is identical for all injectors and it varies as a function of the angle of rotation. For constructive reasons, usually the rail cross-section is constant, causing a pressure drop (and a consequent injected oil flow rate decrease) after each injector.
The oil flow trough the machine has been modeled according to a quasi-steady assumption, being the length of the rail sufficiently reduced, and the speed of sound in oil sufficiently high, to neglect the pressure wave fluctuation (this is also valid for air/oil mixtures in which the speed of sound is significantly reduced).

A simplified sketch of the rail model is reported in Fig.6 in which five injectors have been considered. The oil circuit has been modeled as follows:

a. the oil motion originates from a high pressure plenum at the same pressure as the air being compressed, usually from the separator. A boundary condition which considers the conservation of energy without losses is applied from the separator till section 0_i
b. the filter which usually follows is considered as a simple pressure loss.
c. the remaining circuit is considered as a number of capacities separated from each other by the injectors. The pressure losses between adjacent capacities result from two contributions: the first related to the friction, the second related to the sudden expansion suffered by the oil due to the mass lost through the injectors whilst maintaining a constant rail cross section. This result in a transition from turbulent to laminar flow depending on the value of Re_i
d. The upstream injector pressure is calculated as a result of a simple pressure loss from the adjacent preceeding capacity ($k_{dev,i}$)

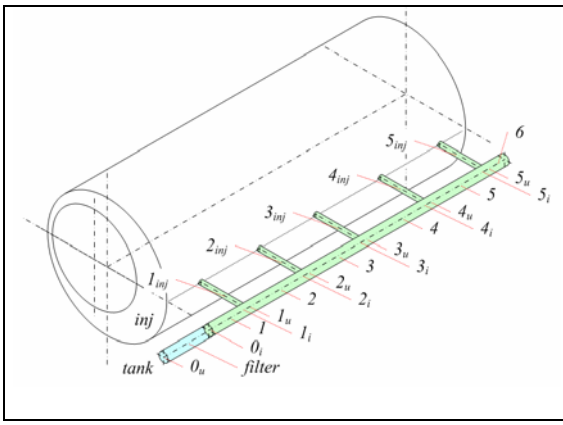

$$
\begin{cases}
P_{i_i} - P_{i_{inj}} = k_{dev_i} \cdot Q_i^2 \cdot \rho / \left(2 \cdot S^2\right) - \left[Q_i^2 / S^2 - Q_{i_{inj}}^2 / S_{inj}^2 \right] \cdot \rho / 2, \ for \ \ i=1..5 \\
P_{i_{inj}} - P_{inj} = \left(k_{outflow_i} - 1\right) \cdot Q_{i_{inj}}^2 \cdot \rho / \left(2 \cdot S_{inj}^2\right), \ for \ \ i=1..5 \\
Q_{i_{inj}} = Q_i - Q_{i+1}, \ for \ \ i=1..5 \\
Q_6 = 0 \\
P_{tank} - P_{0_i} = \left(k_{inf\,low} + 1\right) \cdot Q_1^2 \cdot \rho / \left(2 \cdot S^2\right) \\
P_{0_i} - P_{0_u} = k_{filter} \cdot Q_1^2 \cdot \rho / \left(2 \cdot S^2\right) \\
P_{i-1_u} - P_{i_i} = k_{distr_i} \cdot Q_i^2 \cdot \rho / \left(2 \cdot S^2\right), \ for \ i=1..5 \\
P_{i_i} - P_{i_u} = k_{direct_i} \cdot Q_i^2 \cdot \rho / \left(2 \cdot S^2\right) - \left(Q_i^2 - Q_{i+1}^2\right) \cdot \rho / \left(2 \cdot S^2\right), \ for \ i=1..5 \\
k_{distr_i} = \lambda_i \cdot L_i / D \\
\begin{cases}
\lambda_i = 64 / Re_i, \ if \quad Re_i \le 2100 \\
1 / \sqrt{\lambda_i} = -2 \log \left[2.51 / \left(Re_i \cdot \sqrt{\lambda_i} \right) + \varepsilon / \left(3.71 \cdot D\right) \right], \ if \ \ Re_i > 2100
\end{cases}
\end{cases}
\tag{11}
$$

Fig. 6 – Oil circulation modeling

When the pressure losses are evaluated the model considers the possibility to switch from turbulent to laminar flow depending on the speed reduction of the oil as it proceeds inside the rail. According to these assumptions the equations (11) in Fig 6 apply.

Once all the geometrical aspects have been defined, the upstream pressure at the separator, the cell pressure and the *k* factors are known, the solution of the system of equations gives the overall oil circulation inside the machine as well as the mass flow rate injected inside the cells.

7. TEST BENCH

A specific test bench has been built, Figure 7, in order to measure the more relevant quantities of a SVRC. These include the instantaneous shaft speed and torque, the oil properties (mass flow rates, temperatures, pressure), the air properties (humidity, mass flow rates, inlet and exhaust pressures and temperatures), efficiencies of the heat exchangers related to the specific application (oil and air cooling) and stator temperature maps. The experimental test bench is under improvement by the installation of a continuous piezoelectric pressure measurement inside each compressor cell and optical visualization instrumentation.

8. RESULTS

The SVRC M111D of Ing. Enea Mattei S.p.A. has been tested in order to validate the capabilities of the comprehensive model to represent the phenomena. The M111D is a machine designed to give 2690 l/min @ 7.5 bar while absorbing 17 kW. Like most SVRCs of this size it is designed with an integrated separation system to allow the compressor unit to be easily coupled to any driving equipment (electric motor, diesel engine, hydraulic motor, etc…) it is one of the highest selling machines in the Mattei SVRC compressor range therefore it was chosen as the first test subject for the simulation/experimental comparison.

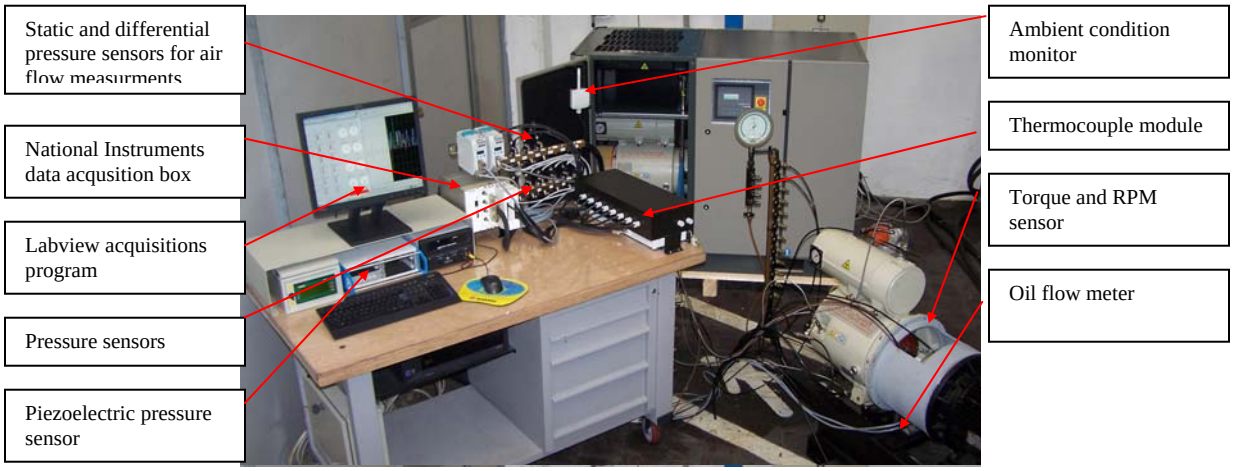

Figure 7 – Test bench

The M111D SVRC has been tested in a wide range of situations (design and off design) in order to strengthen some phenomena with respect to the others and observe the effects on the more relevant quantities influencing the performances of the compressor.
In figure 8 the theoretical results are shown concerning the p-V diagram with a severe throttling at the intake section and in a normal situation (unthrottled). The induction in the first case is below the ambient pressure (0.3 bar) producing a strong reduction of the FAD without a correspondent decrease in the power absorbed.

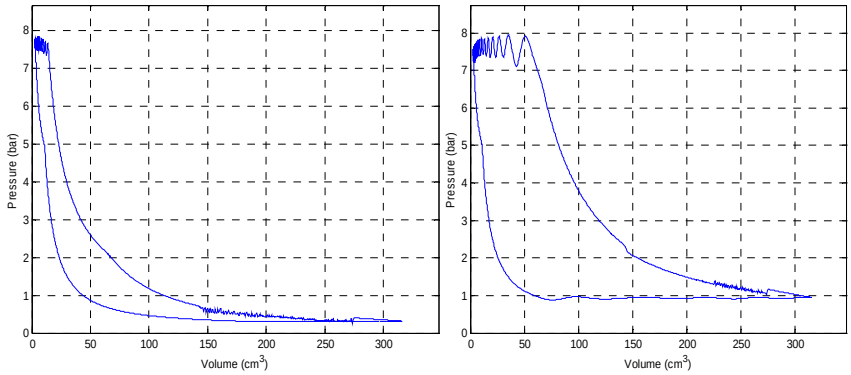

Figure 8 – p-V diagram: throttled intake (left), unthrottled (right)

Figure 9 and Figure 10 show the comparison between measured and calculated data concerning the FAD the torque respectively as a function of machine RPM. Three situations are shown referred to different values for the pressure of the air delivered. The following aspects can be outlined:

a) the FAD is very well represented by the model: in the worst cases, differences of (5-7) % are present in the direction of overestimating the real FAD at low shaft speed and underestimating it as the shaft speed increases;
b) the prediction of the shaft torque requires a fine representation of the friction between blades and stator surfaces; nevertheless, the capability of equation (9) is still enough to give a torque estimation inside an error range of the order of 25% ; for the lower values of the pressure delivered (7.5 bar, 9.5 bar) the agreement is more satisfactory (the error falls inside a 10%-20% range) as the shaft speed increases; when the pressure delivered increases (12.5 bar) a constant difference between experimental and theoretical values appears in which the prediction is always underestimated compared to the experimental values. These results have been reached for a fixed value of the friction coefficient. A fine tuning has been performed by considering the friction coefficient pressure dependent (and also shaft speed dependent): in this case the error decreases to within a 7.5 % range. These results are not included since this more complex representation is still being researched.

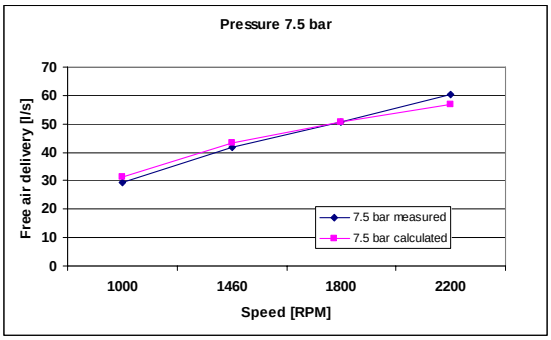

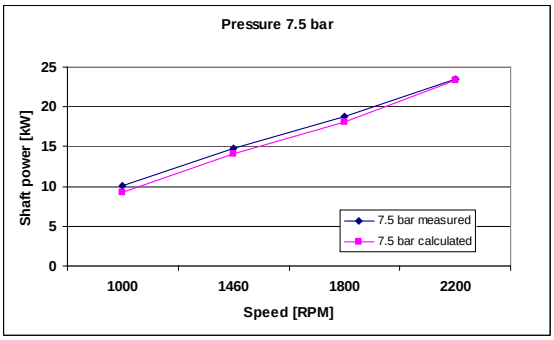

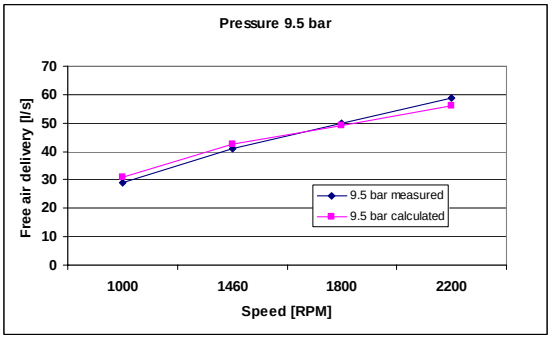

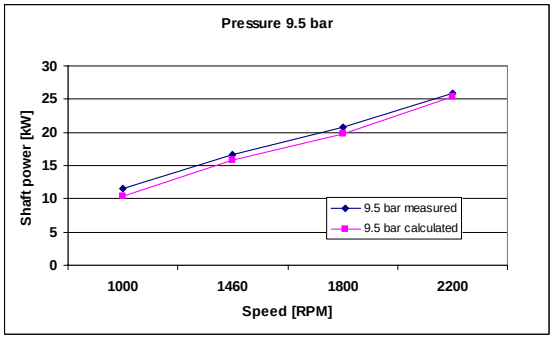

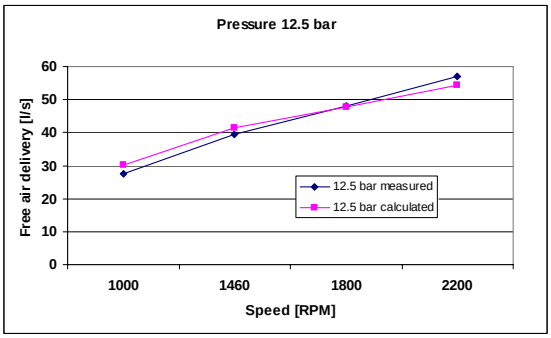

Figure 9 – FAD as a function of RPM

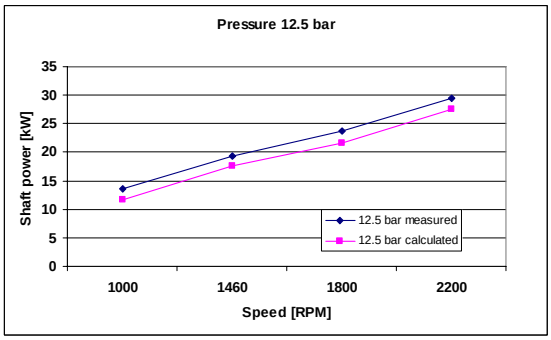

Figure 10 – Shaft power as a function of RPM

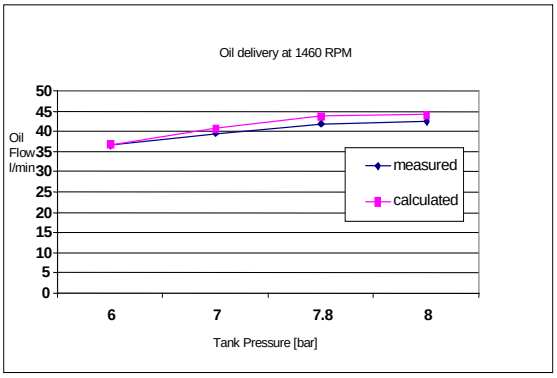

Figure 11 – Oil circulation

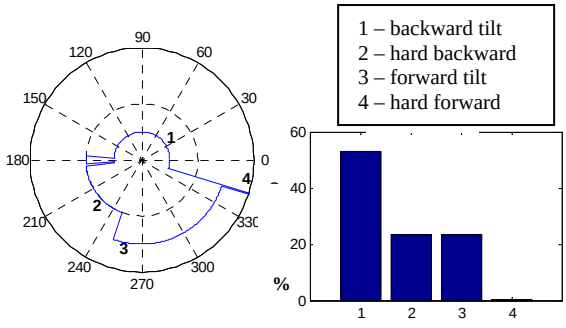

Figure 12 – Blade setting

A comparison concerning the oil dynamics inside the machine is reported in Figure 11: the agreement is quite satisfactory considering the relative complexity of the modeling, equations (11). The data has been calculated using literature data for pressure losses and transitional regimes and the total mass flow rate is a result of adding the six mass flow rates which correspond to the five injectors. This agreement also shows a good representation of the pressure inside the cell, this is the backpressure in the injection process.

The blade setting inside the slot is shown in figure 12: it shows the angular persistence of the states during rotor motion. Observing the bar chart, state 1 is the most frequent (it extends for 55 angular degrees), while state 2 and 3

have more or less the same persistency (25 angular degrees). It is important to remark that the model predicts a high frequency transition between the four states which could explain some wear around the lateral surfaces of the blades.

9. CONCLUSIONS

A comprehensive model of a SVRC was presented representing with respect to [1] an evolution which takes into account oil circulation inside the machine, blade vibration inside the slots and the power absorbed due to friction.
Various arrangements, including frontal or lateral suction ports, circular and non-circular stators, and radial or non-radial blades characterize the geometrical model; a detailed fluid dynamics description based on the QPM has been adopted to represent the mass flow rates exchanged with the environment and toward the discharge line, catching all the transient phenomena involved (capacitive, inertial, propagative). The thermal aspects are also characterized. The oil circulation model allows for the calculation of the oil injected from each injector and it interacts with the thermodynamic situation inside the cells. The position of the blade inside the slots is calculated according to the equilibrium of the forces applied to the blade as well as the reaction forces which allows for the calculation of the power loss caused by friction. A test bench has been built to validate the model; comparisons in terms of FAD, torque and oil circulation have been made between theoretical and experimental data. The quality of the agreement demonstrates the capability of the overall modeling to physically represent the complex behavior of a SVRC and the full validity of the model as a design tool. This work has allowed the authors to adopt this software as a design tool when developing innovative solutions in the rotary vane compressor industry.

APPENDIX ($F_{bp} = -B_1 l \Delta p$)

Backward tilt

$$A = \begin{bmatrix} \mu\text{sign}(\vartheta) & \mu\text{sign}(\vartheta) & \mu\sin\vartheta - \cos\vartheta \\ 1 & -1 & -\mu\cos\vartheta - \sin\vartheta \\ 0 & L_1 - \mu b\text{sign}(\vartheta) & -\mu L_2\cos\vartheta - \mu B_1\sin\vartheta - L_2\sin\vartheta + B_1\cos\vartheta \end{bmatrix}; \quad B = \begin{bmatrix} F_{bp} + F_c \\ -F_{pn} \\ -F_{pn}L_2/2 - F_{bp}B_1 - F_cB_1 \end{bmatrix}$$

Hard backward

$$A = \begin{bmatrix} \mu\text{sign}(\vartheta) & \mu\text{sign}(\vartheta) & \mu\sin\vartheta - \cos\vartheta \\ 1 & 1 & -\mu\cos\vartheta - \sin\vartheta \\ 0 & -L_1 & -\mu L_2\cos\vartheta - \mu B_1\sin\vartheta - L_2\sin\vartheta + B_1\cos\vartheta \end{bmatrix}; \quad B = \begin{bmatrix} F_{bp} + F_c \\ -F_{pn} \\ -F_{pn}L_2/2 - F_{bp}B_1 - F_cB_1 \end{bmatrix}$$

Forward tilt

$$A = \begin{bmatrix} \mu\text{sign}(\vartheta) & \mu\text{sign}(\vartheta) & \mu\sin\vartheta - \cos\vartheta \\ -1 & 1 & -\mu\cos\vartheta - \sin\vartheta \\ 0 & -L_1 + \mu b\text{sign}(\vartheta) & -\mu L_2\cos\vartheta + \mu B_1\sin\vartheta - L_2\sin\vartheta - B_1\cos\vartheta \end{bmatrix}; \quad B = \begin{bmatrix} F_{bp} + F_c \\ -F_{pn} \\ -F_{pn}L_2/2 + F_{bp}B_1 + F_cB_1 \end{bmatrix}$$

Hard forward

$$A = \begin{bmatrix} \mu\text{sign}(\vartheta) & \mu\text{sign}(\vartheta) & \mu\sin\vartheta - \cos\vartheta \\ -1 & -1 & -\mu\cos\vartheta - \sin\vartheta \\ 0 & L_1 & -\mu L_2\cos\vartheta + \mu B_1\sin\vartheta - L_2\sin\vartheta - B_1\cos\vartheta \end{bmatrix}; \quad B = \begin{bmatrix} F_{bp} + F_c \\ -F_{pn} \\ -F_{pn}L_2/2 + F_{bp}B_1 + F_cB_1 \end{bmatrix}$$

REFERENCES

(1) Cipollone R., Contaldi G., Sciarretta A., Tufano R., *A comprehensive model of a sliding vane rotary compressor system*, ImechE International conference on compressors and their systems 2005, pp 195-205
(2) Tramschek A.B. and M.H. Mkumbwa, *Mathematical Modelling of Radial and Non-radial Vane Rotary Sliding Vane Compressors*, Proc. of the 1996 International Compressor Conference at Purdue, pp. 477-484.
(3) Hanton J., *Machines voluètriques à palettes* (in French), Revue-M Mèchanique, vol. 28, no. 2, pp. 91-101, 1982.
(4) Vaisman I.B., *Computer aided functional design principles of rotary vane compressors*, ImechE International conference on compressors and their systems 1999, pp. 599-608
(5) Tramschek A.B. and M.H. Mkumbwa, *Experimental Studies of Non-Radial Vane Rotary Sliding Vane Air Compressors During Steady State Operation*, Proc. of the 1996 International Compressor Conference at Purdue, pp. 485-492.
(6) Cipollone R. and A. Sciarretta, *The Quasi-Propagatory Model: a New Approach for Describing Transient Phenomena in Engine Manifolds*, SAE Technical paper no. 2001-01-0579.